THE JOURNAL OF PHYSICAL CHEMISTRY A

Article

Cite This: J. Phys. Chem. A 2019, 123, 9069−9078

pubs.acs.org/JPCA

Blue Phosphorescent *trans*-N-Heterocyclic Carbene Platinum Acetylides: Dependence on Energy Gap and Conformation

James D. Bullock,[†,§] Silvano R. Valandro,[‡,§] Amanda N. Sulicz,[‡] Charles J. Zeman, IV,[†,‡] Khalil A. Abboud,[†] and Kirk S. Schanze*[,‡]

[†]Department of Chemistry, University of Florida, Gainesville, Florida 32611, United States

[‡]Department of Chemistry, University of Texas at San Antonio, One UTSA Circle, San Antonio, Texas 78249, United States

Supporting Information

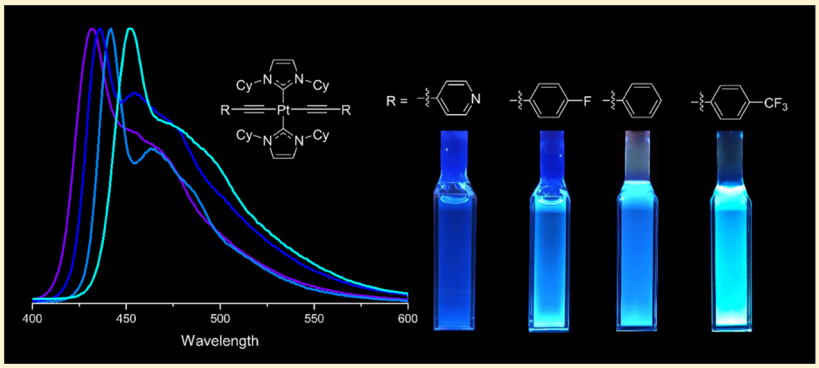

ABSTRACT: A series of 11 complexes of the type *trans*-$(NHC)_2Pt(CC\text{-}Ar)_2$ (where NHC = N-heterocyclic carbene) have been synthesized and their photophysics characterized. The complexes display moderately efficient deep blue to green phosphorescence from a triplet excited state that is localized mainly in the aryl acetylide ligand (CC-Ar). The emission energy varies with the substituent on CC-Ar, with the highest energy emission for Ar = 4-pyridyl. The emission quantum efficiency and lifetime for the series decreases with increasing emission energy (E_{em}), and the effect is identified as arising from an increase in the nonradiative decay rate (k_{nr}) with E_{em}. Temperature-dependent emission lifetime studies for three complexes give activation energies for the nonradiative decay process ∼1000 cm^{-1}, and the thermally activated decay process is attributed to crossing to a nonemissive metal-centered (d−d) excited state. At a low temperature, two different emission progressions are observed. Density functional theory calculations suggest that the triplet energy varies with the torsion of the aryl acetylide rings relative to the plane defined by the PtC_4 unit (where C = the carbon atoms bonded to Pt). The multiple emission is ascribed to emission from complexes differing with respect to the aryl acetylide ring torsion. Ultrafast transient absorption spectroscopy reveals a fast relaxation (∼5 ps) that may also be due to aryl acetylide ring torsional relaxation in the triplet excited state.

INTRODUCTION

Over the last 2 decades, platinum acetylide complexes, oligomers, and polymers have attracted increasing attention owing to their rich photophysical properties.[1−8] Engineering the structure and, consequently, the photophysical properties of these organometallic systems have led to potential applications that include nonlinear absorption,[9−12] organic light-emitting diodes (OLEDs),[13−15] optical limiting materials,[16,17] and photovoltaic devices.[18−20] The basis of the successful utilization of platinum acetylides in these applications is the strong interaction through orbital overlap among aryl acetylide ligands with the large spin−orbit coupling heavy metal, which results in an efficient intersystem crossing to a long-lived triplet excited state combined with strong phosphorescence. These properties open the path for bimolecular diffusion-controlled excited state chemistry and OLED technologies.

Since the first report of platinum(II) acetylide complexes bearing phosphine ligands by Chatt and Shaw in 1959,[21] intensive research in the design and study of the photophysical properties of these complexes has been reported.[1−8] However, most of the previously studied complexes are not viable candidates for OLED application due to their long triplet lifetimes and generally low quantum yields. Additionally, the use of phosphine ligands generally does not allow for the display of blue emission due to the presence of a low-lying metal-centered state.[1] To circumvent this problem, efforts have been made to enhance the yield of phosphorescent emitters through the use of strong-field ligands, such as N-heterocyclic carbenes (NHCs). The strong σ-donating ability of NHCs can serve an effective means to banish metal-centered d−d states

Received: July 24, 2019
Revised: September 18, 2019
Published: September 22, 2019

DOI: 10.1021/acs.jpca.9b07079
J. Phys. Chem. A 2019, 123, 9069−9078

Chart 1. Synthesized Complexes

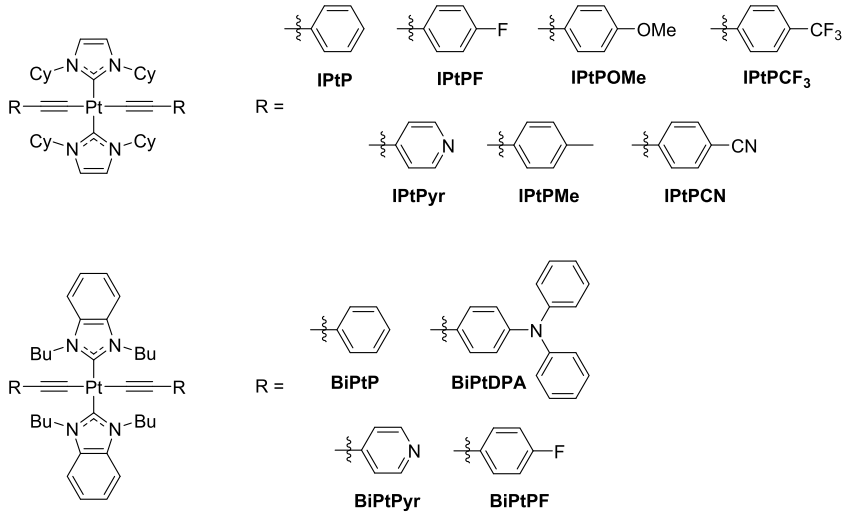

Scheme 1. General Synthetic Strategy

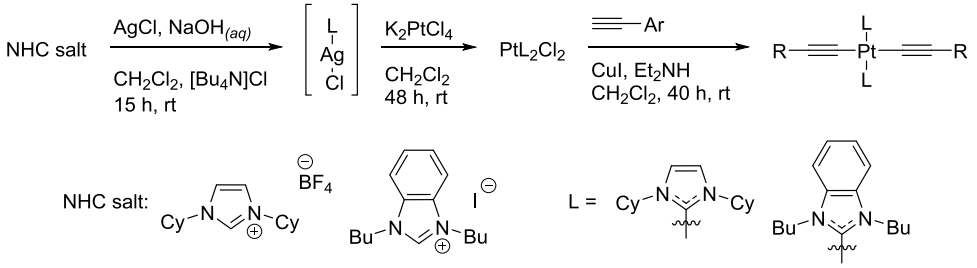

so high in energy that it renders them thermally inaccessible.[22,23] The first platinum(II) carbene complex was derived from an isocyanide in 1969.[24] Later work involving platinum(II) carbene complexes has included an acetylacetonato (acac) cyclometalating ligand.[25,26] More recently, work conducted by the Venkatesan[14,27,28] and Schanze[29] groups combined the strong σ-donating nature of the NHC with acetylide ligands, providing examples of NHC platinum(II) acetylides, which are candidates as deep blue phosphorescent emitters.

The work described here expands the library of possible *trans*-NHC Pt(II) acetylides. The main objective of the work described herein is the synthesis and structural characterization of the complexes and the characterization of their photophysics. Some of the complexes reported here were previously reported by others, but the synthetic pathways here are improved, and the detailed photophysical investigation is new.[14,30]

Importantly, we have developed a general synthetic strategy that involves a transmetalation step to complex the carbene ligands onto platinum(II). We have also explored the photophysical properties including the absorption, emission, and transient absorption, with some experiments carried out at variable temperature. These results reveal an interesting dependence of the emission efficiency and lifetime on the energy of the phosphorescent state, suggesting the involvement of a thermally activated crossing to a nonemissive, metal-centered excited state. Finally, low-temperature phosphorescence and transient absorption studies suggest that there is a conformational relaxation that occurs following excitation and intersystem crossing, and this may be related to differences in the lowest-energy conformations of the singlet ground and triplet excited states (Chart 1).

RESULTS

Synthesis and Characterization. The general synthetic scheme for the *trans*-N-heterocyclic carbene (NHC) platinum(II) acetylides is shown in Scheme 1. In the first step, the imidazolium salt is deprotonated, then ligated to Ag(I). Upon removal of the aqueous layer, the *trans*-NHC platinum(II) dichloride precursor is formed through transmetalation of the Ag(I)−NHC complex with K_2PtCl_4 to afford *trans*-$(NHC)_2PtCl_2$. The acetylide ligands are then added under Hagihara conditions to give the desired *trans*-NHC platinum(II) acetylide. The synthesis of the methoxy-substituted acetylide was more efficient when deprotonation was done with the use of *n*-butyl lithium. For synthesis of the *trans*-benzimidazole $Pt(II)Cl_2$ starting material, three equivalents of benzimidazole (BIm), instead of two, were used, which significantly enhanced the yield from 10 to 95%.[14] Additional modifications, including mild reaction conditions and increased scalability, were made to the syntheses of the acetylide complexes from previous reports.[14,30] The syntheses reported here also only show the presence of the *trans*-isomer, with significantly increased yields from previous reports, 30−90%, depending on the choice of acetylide ligand.[14] Specific optimizations for each reaction are reported in the Supporting Information.

Structures of the complexes were confirmed by ^{1}H NMR, ^{13}C NMR, and high-resolution mass spectrometry (Supporting Information). The *trans* geometry of IPtP and BiPtP was confirmed by X-ray crystallography, and the structural metrics

DOI: 10.1021/acs.jpca.9b07079
J. Phys. Chem. A 2019, 123, 9069−9078

are in good agreement with previous reports.[14] The *trans* geometries for the other acetylides were confirmed by ^{1}H NMR. Consistent with previous reports, these complexes displayed a single multiplet for the H's α- to the NHC nitrogen (~5.4 ppm for the imidazole (Im) and 4.9 ppm for the benzimidazole species), where the *cis*-isomer displays two multiplets.[14] Each of the NHC platinum(II)-acetylide derivatives shows consistent integration, chemical shift, and splitting associated with the carbene ligand when compared to the parent complex, either IPtP or BiPtP.

Photophysical Properties. The UV−visible absorption and photoluminescence spectra for a selected set of *trans*-NHC platinum(II) acetylides in tetrahydrofuran (THF) at room temperature are shown in Figure 1. Spectra for the remaining series of complexes are shown in Figures S40 and S41 (Supporting Information). A summary of photophysical properties, including emission lifetimes, quantum yields, and calculated decay rates, for all of the complexes is shown in Table 1.

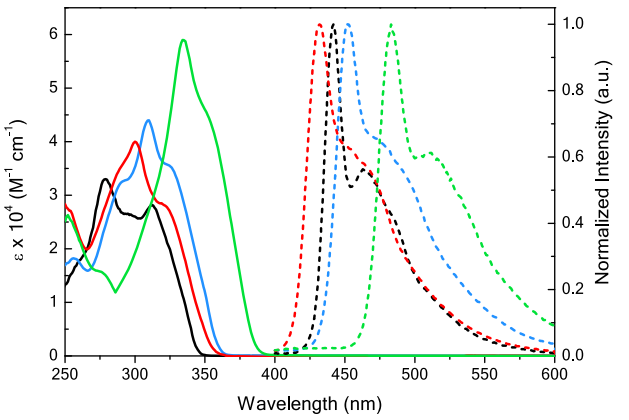

Figure 1. Absorption (solid lines) and normalized emission (dashed lines) spectra for platinum(II) acetylides with imidazole carbene ligand in THF under argon atmosphere. Black trace corresponds to IPtP, IPtPyr in red, IPtPCF$_3$ in blue, and IPtPCN in green. Absorption is plotted as a function of molar absorptivity (ε).

The absorption spectrum of each platinum(II) acetylide complex is dominated by a strong band at 275−345 nm with molar extinction coefficients in the range of (3.1−6.0) × 10^4 M^{-1} cm^{-1} in THF. Based on previous density functional theory (DFT) calculations, these bands can be assigned mainly to ligand centered $\pi \rightarrow \pi^*$ transitions (LC) with a minor contribution from metal-to-ligand charge transfer (MLCT).[13] The absorption characteristic for each complex in THF is dependent on the identity of the NHC ligand. The complexes featuring benzimidazole carbene ligand (Figure S41) exhibited larger molar extinction coefficients compared to the corresponding imidazole complexes, apparently due to the expanded π-system in the benzimidazole ring. The Pt complexes also feature photoluminescence emission with a maximum at 431−483 nm and emission lifetimes of the order of microseconds (Table 1). On the basis of the large Stokes shifts (>100 nm), the moderate emission lifetimes, and the quenching of the emission by oxygen in the air, this photoluminescence emission can be assigned to phosphorescence.

As shown in Figure 1, the positions of the absorption and phosphorescence bands are dependent on the nature of the substituent group on the phenyl acetylide ligands. Electron-withdrawing groups lead to a red-shift in both absorption and phosphorescence spectra in comparison to the unsubstituted phenyl acetylide ligand. On the other hand, electron-donating groups result in a slight red-shift in absorption without a significant change in phosphorescence.

From a close analysis of the results in Table 1, it is possible to discern a clear trend in the variation of the phosphorescence quantum yield and lifetimes (Φ_{ph} and τ, respectively) with emission energy (E_{em}). Specifically, both Φ_{ph} and τ generally decrease as E_{em} increases. By measuring the phosphorescence emission lifetime (τ) and the quantum yield (Φ_{ph}), the rates of the nonradiative (k_{nr}) and radiative decay (k_r) of the excited state are calculated by using the following equations

$$k_{nr} = 1/\tau \text{ and } k_r = \Phi_{ph}/\tau \quad (1)$$

As can be seen from the data in Table 1, the radiative rates vary only slightly across the family of complexes; however, the nonradiative rates vary significantly, with more than a 100-fold increase with increasing emission energy.

Figure 2 shows more clearly the correlation between the nonradiative decay rate and emission energy. Here, it is easily seen that there is a general trend of increasing nonradiative decay rate with emission energy. Although the trend is not quantitatively linear, there clearly is a general correlation of increasing ln k_{nr} with E_{em}.[31] From this behavior, we infer that there is likely a nonemissive (metal-centered d−d) state that

Table 1. Photophysical Properties of Platinum(II) Acetylide Complexes

compound	$\lambda_{max(abs)}$[a] (nm)	ε[a] (M^{-1} cm^{-1})	$\lambda_{max(em)}$[b] (nm)	Φ_{ph}[cc]	τ[d] (μs)	k_r (10^4 s^{-1})	k_{nr} (10^5 s^{-1})	E_{em}[e] (eV)
IPtPyr	300	40 000	432	0.012	0.10	12	99	2.87
IPtPF	275	28 000	436	0.04	2.1	1.9	4.6	2.84
IPtPOMe	282	31 000	441	0.06	1.1	5.5	8.5	2.81
IPtPMe	278	31 000	442	0.065	3.7	1.6	2.5	2.80
IPtP[13]	279	33 000	444	0.029	1.7	1.8	5.7	2.79
IPtPCF$_3$	310	44 000	452	0.19	5	3.8	1.6	2.74
IPtPCN	334	59 000	483	0.45	39	1.1	0.14	2.57
BiPtPyr	291	52 000	431	0.012	0.35	3.4	28	2.88
BiPtPF	282	45 000	435	0.06	1.4	4.3	6.7	2.85
BiPtP	289	46 000	438	0.08	1.8	4.4	5.1	2.83
BiPtPDPA	345	67 000	483	0.12	36	0.33	0.24	2.57

[a]Measured in THF. [b]Measured in argon bubble-degassed THF. [c]Measured in argon bubble-degassed THF with respect to Ru(bpy)$_3$Cl$_2$ (Φ = 0.038) in aerated deionized water. [d]Measured by time-correlated single-photon counting (TCSPC) in argon-degassed THF. The error of quantum yields is estimated to be approximately 10%. [e]The emission energies were calculated from the λ_{max}(em).

DOI: 10.1021/acs.jpca.9b07079
J. Phys. Chem. A 2019, 123, 9069−9078

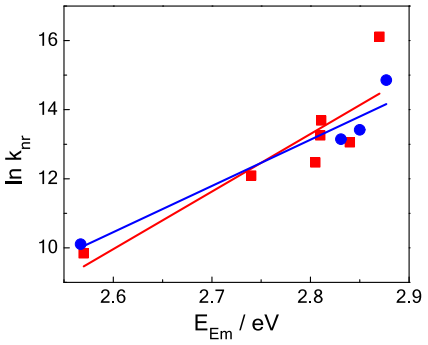

Figure 2. Correlation between the nonradiative decay rate (ln k_{nr}) as a function of emission energy for imidazole (■) and benzimidazole (●) platinum(II) acetylide complexes. The regression lines have slopes of 17.8 ± 3.9 and 13.4 ± 2.5 eV^{-1} for imidazole and benzimidazole, respectively.

lies at higher energy relative to the emitting state that provides a pathway for rapid nonradiative decay.[32,33] This point will be explored more fully below through temperature-dependent emission experiments.

Temperature-Dependent Emission. To provide more insight regarding the excited-state dynamics, the temperature dependence of the emission spectra for a selected set of complexes including IPtP, IPtPCF$_3$, IPtPCN, and IPtPyr was studied over the temperature range from 80 to 300 K in 2-methyltetrahydrofuran (MTHF) solvent/glass. Figure 3 shows the phosphorescence emission as a function of temperature for IPtP, while the spectra for the other Pt complexes are included in the Supporting Information (Figures S42−S44).

There are several interesting features associated with the temperature-dependent emission spectra for the *trans*-NHC platinum(II) acetylides. As shown in Figure 3a,b, when the temperature is above 120 K, the emission appears as a single 0-0 band with vibronic progression at lower energy. By contrast, at a lower temperature (<90 K), an additional 0-0 band at a shorter wavelength was observed for all four complexes (see Figures S42−S44). The presence of two emission onsets in the frozen solvent glass is likely due to nonequilibrating conformers that have different emission energies. As the solvent viscosity decreases with the increasing temperature, conformational relaxation is possible, and only single emission progression is observed. Similar observations were reported for complexes of the type *trans*-Pt$(PR_3)_2(CC\text{-}Ar)_2$ and attributed to conformers arising from rotations of the aryl acetylide ligands.[34] Figure 3d shows that it is possible to use excitation wavelength to photoselect the emission from the two different conformers at a low temperature (80 K). In particular, with 278 nm excitation, the emission envelope is dominated by the progression with the short-wavelength 0-0 band, whereas with excitation at 340 nm, the emission is dominated by the progression that has its onset at a longer wavelength. This behavior suggests that the conformers have different absorption spectra, and by varying excitation wavelength, it is possible to selectively excite a specific conformer.

The phosphorescence quantum yield (Φ_{ph}) also changes significantly with the temperature. Starting at 77 K, Φ_{ph} increases with temperature, reaching a maximum in the range 120−220 K, depending on the substituent group on the phenyl acetylene ligands (Figures 3c and S42−S44). Once Φ_{ph} reaches a maximum, it generally decreases with the increasing temperature to room temperature. The trend of decreasing Φ_{ph} with the increasing temperature suggests the existence of a low-lying triplet metal-centered excited state (^{3}MC) that lies above the emitting $^3\pi,\pi^*$ state that can be thermally populated at higher temperatures.[33,35]

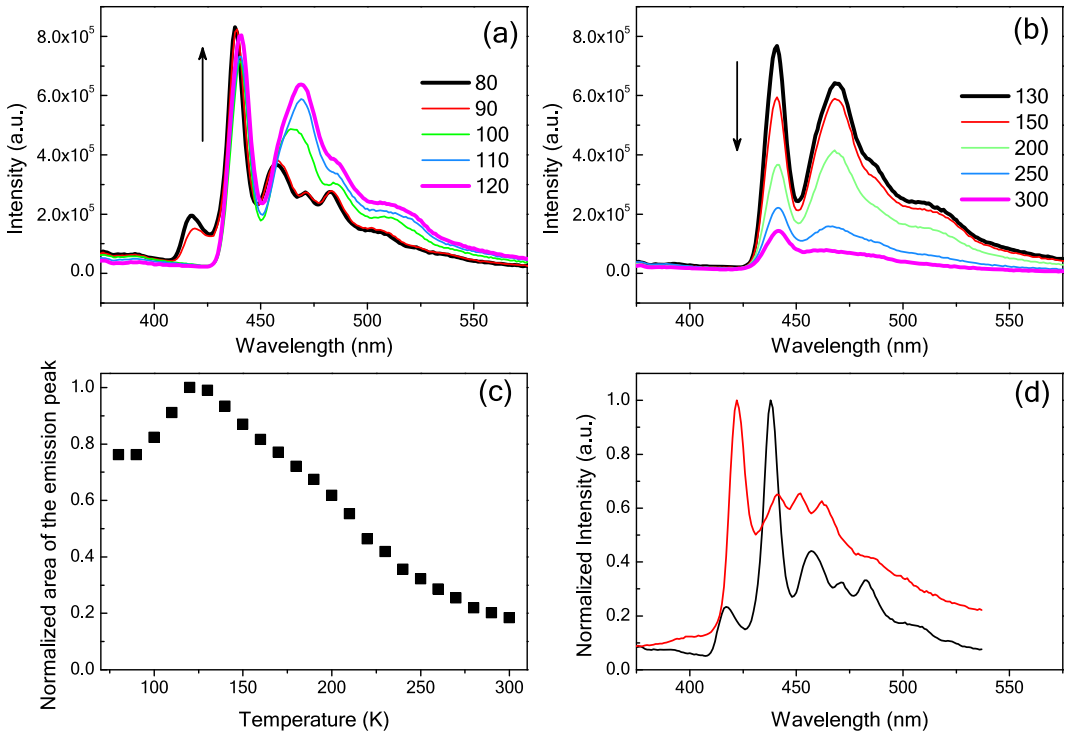

Figure 3. Photoluminescence of IPtP in MTHF solvent glass. (a) Spectra from 80 to 120 K and (b) from 130 to 300 K, λ_{ex} = 340 nm. (c) The normalized area under the emission spectra vs temperature. (d) Emission spectra at 80 K with excitation at 278 nm (red) and 340 nm (black).

DOI: 10.1021/acs.jpca.9b07079
J. Phys. Chem. A 2019, 123, 9069−9078

To obtain more information on the excited-state dynamics underlying the temperature dependence of the emission yields, temperature-dependent emission lifetime (τ_{em}) measurements were carried for IPtPCN, $IPtPCF_3$, and IPtPyr. These experiments were carried out over the temperature range 80−290 K in the MTHF solvent. The temperature-dependent lifetime data was fitted by using a modified Arrhenius equation, eq 2.

$$k_d(T) = k_0 + k_1 e^{(-E_a/RT)} \quad (2)$$

Equation 2 assumes that the total excited-state decay rate ($k_d = 1/\tau_{em}$) comprises a temperature-independent rate (k_0) and a temperature-dependent pathway with activation energy (E_a) and pre-exponential (k_1).[32,36] This treatment has been used to analyze the temperature dependence of the total excited-state decay rate of a variety of transition-metal complexes, including $Ru(bpy)_3^{2+}$, where the emissive metal-to-ligand charge-transfer excited state decays via thermally activated crossing to a metal-centered (dd) excited state.[33,35] In these treatments, the temperature-independent term (k_o) has been attributed to the sum of the temperature-independent radiative and non-radiative rates of the emissive state, and k_1 is the relaxation rate of the dark state. We assume a similar interpretation of the parameters extracted from the analysis via eq 2.

Figure 4 displays plots of the emission lifetime data as ln k_d vs T for IPtPCN, $IPtPCF_3$, and IPtPyr over the 80−295 K range (where $k_d = 1/\tau_{em}$). Overall, it is clear that the emission decay rate (k_d) of each complex generally increases with temperature. We also observe that below the solvent melting point, the emission decay rate modestly changes. Table 2 contains the parameters obtained from the nonlinear regression analysis of the temperature dependence data for IPtPyr, $IPtPCF_3$, and IPtPCN according to eq 2 (see Figure S45 for fits). IPtPyr has the smallest E_a value followed by $IPtPCF_3$ and IPtPCN. Although the difference in the E_a values is comparatively small, the trend is that E_a increases as E_{em} decreases.

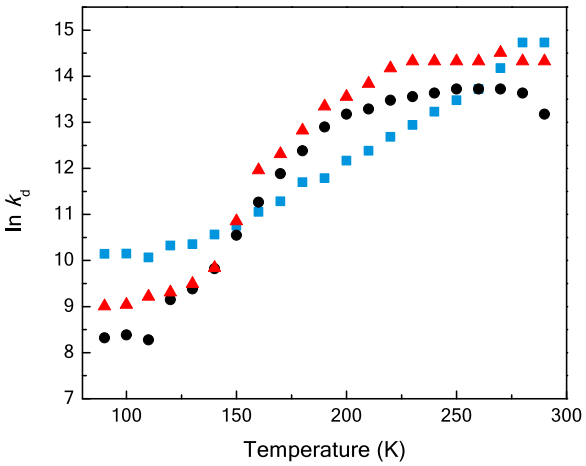

Figure 4. Temperature dependence of the excited-state decay rate (k_d) in 2-methyl THF for IPtPyr(■), IPtPCN (▲), and $IPPCF_3$ (●).

Table 2. Kinetic Parameters Obtained from the Analysis of the Temperature Dependence of the Emission Decay[a]

compound	k_0 (s^{-1})	k_1 (s^{-1})	E_a (cm^{-1})
IPtPyr	2.5×10^4	5.6×10^7	810
$IPtPCF_3$	6.3×10^3	4.0×10^9	1160
IPtPCN	4.7×10^3	3.3×10^9	1200

[a]Kinetic parameters, as defined in eq 2. See Figure S45 for fits to the experimental data.

Ultrafast Transient Absorption Spectroscopy. Transient absorption difference spectra of IPtP and $IPtPCF_3$ in the THF solution over the time scale of 750 fs to 7 ns were measured, and the results are shown in Figure 5. Transient absorption spectra for several other *trans*-NHC platinum acetylide complexes are included in the Supporting Information (Figure S46). Two prominent features are common to the spectra for all of the complexes over the fs−ns time scale: immediately following the 330 nm excitation pulse, an absorption band in the visible region appears, which slightly increases in intensity and shifts to a longer wavelength over first 25 ps. The dynamics of this fast time scale process is shown in the insets in Figure 5. Following these initial fast spectral changes, the transient absorption spectrum decays (ca. 20%) uniformly up to the longest delay time measured (8 ns). Importantly, at longer time delays (t > 50 ps), the band closely resembles in shape and wavelength maximum the visible region nanosecond transient absorption and, therefore, can be ascribed to a long-lived triplet state (for comparison, the ns−μs transient absorption spectrum of $IPtPCF_3$ was recorded, Figure S47. Unfortunately, our ns−μs transient absorption system does not allow excitation below 355 nm, and this limited the number of complexes that could be probed on the longer time scale).

The spectral dynamics observed in the first 25 ps of the transient absorption may correspond to conformational relaxation in the triplet excited state, possibly related to rotations of the phenylene and/or carbene ligands. Urbas and co-workers[37] reported similar spectra and dynamics for a phosphine-substituted platinum acetylide, *trans*-$Pt(PBu_3)_2(CC\text{-}Ph)_2$. In their work, it was suggested that the triplet state is fully populated within less than 100 fs, and an approximately 5 ps spectral dynamics process is due to structural relaxation of the triplet excited state. These spectral dynamics are in good agreement with the findings reported herein, supporting the suggestion that the growth that occurs on the 25 ps time scale for the carbene complexes is related to conformational relaxation in the triplet state.

Computational Results: Structure of the Ground and Excited States. Density functional theory (DFT) calculations were applied to provide additional insight regarding the relationship between molecular structure and energetics in the ground and triplet excited states of IPtP. Details concerning the computational methods used are provided in the Experimental Section. To simplify the calculations, the N-cyclohexyl substituents on the carbene ligands were replaced with methyl ($-CH_3$) groups.

First, the geometry-optimized structures of the ground (S_0) and first triplet excited (T_1) states for IPtP were computed, and the resulting structures are shown in Figure 6. By taking the difference between the energies of the geometry-optimized S_0 and T_1 structures (e.g., $\Delta E = E(T_1) - E(S_1)$), the adiabatic triplet energy of IPtP was determined to be ΔE = 2.83 eV.[34] This corresponds to a phosphorescence 0-0 wavelength of 438 nm, in excellent agreement with the experimental value (444 nm). There are two main differences between the geometry-optimized S_0 and T_1 structures. First, there is a small contraction in the dihedral angle defined by the orientation

DOI: 10.1021/acs.jpca.9b07079
J. Phys. Chem. A 2019, 123, 9069−9078

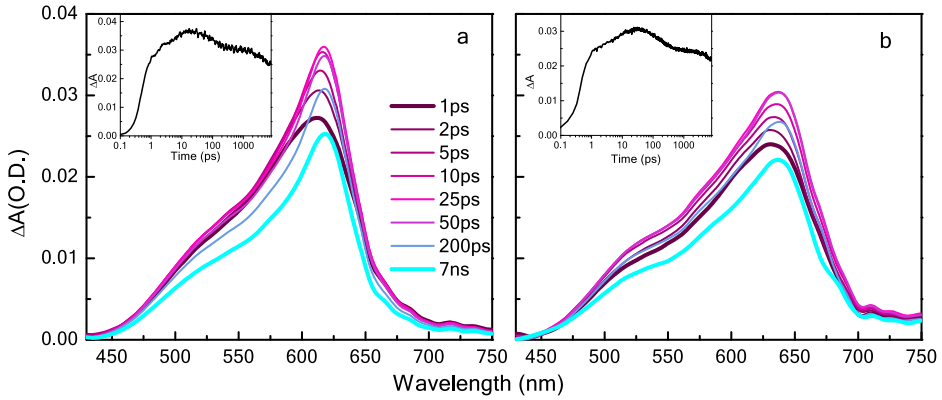

Figure 5. Femtosecond transient absorption spectra of IPtP (a) and IPtPCF$_3$ (b) in THF with 330 nm and 100 μJ excitation. Inset: Kinetic traces of IPtP at 620 nm and IPtPCF$_3$ at 635 nm.

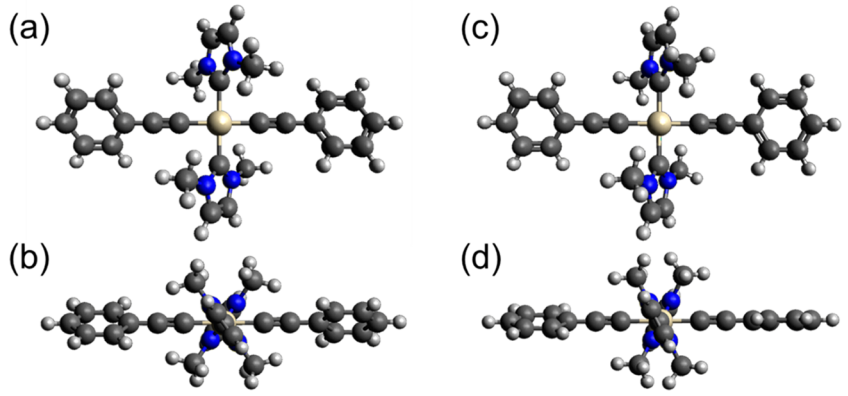

Figure 6. Optimized ground-state geometry (a and b) and excited-triplet-state geometry (c and d) of IPtP from two different viewpoints. For (a) and (c), the view is perpendicular to the PtC$_4$ plane, and for (b) and (d), the view is along the C−Pt−C axis, where C corresponds to the carbene carbon of the imidazole ligand.

of the two imidazole rings (compare Figure 6b,d). Second, and possibly more important, is the fact that the dihedral angles between the planes defined by the phenylene rings and the plane defined by the PtC$_4$ "core" (where C is the four carbon atoms bonded to Pt) are much smaller in T$_1$ compared to S$_0$ (compare Figure 6c,d). A similar preference for this "planar" conformation in the T$_1$ state was found in previous DFT calculations on related Pt−acetylide complexes.[34]

To better understand the relationship between the torsion of the phenylene units and energy in the S$_0$ and T$_1$ states, a "relaxed torsional scan" was carried out.[38] In this calculation, the energy as a function of the relative torsional orientation of the phenylene units was computed in both the S$_0$ and T$_1$ states. In this calculation, the dihedral angle between the phenylene rings was constrained (and incremented); however, the torsion of the phenylene units relative to the plane defined by the PtC$_4$ core was unconstrained. As such, if it is energetically favorable, one phenylene ring will maintain fixed dihedral orientation (relative to the plane of the PtC$_4$ core), while the other ring rotates according to the incremented inter-ring torsional angle. The results of the torsional scan are shown in Figure 7.

There are several important findings from this computational scan. First, in general, it is seen that the energy barrier for rotation of the phenylenes is quite low in the ground state (S$_0$) indicating that the phenylene ligands rotate freely at room temperature. In addition, note that both rings are out of plane relative to PtC$_4$, indicating that the energy does not vary much with the dihedral angle between either phenylene or the PtC$_4$ plane. Second, in contrast to the behavior in the ground state, in the T$_1$ state during the torsional scan, one of the phenylene rings maintains coplanar orientation relative to the PtC$_4$ core, while the other phenylene ring rotates. The barrier to rotation of the second ring is higher than that in the ground state (1.1 kcal/mol); however, it is still relatively a low-energy barrier process. Third, geometries for the T$_1$ state calculated with symmetry constraints give more insight into the effect of phenylene conformation on the triplet energy (Figure S39). In particular, comparison of the energy of the T$_1$ with C_{2v} symmetry (one phenylene in-plane with PtC$_4$, one perpendicular to PtC$_4$, 2.29 kcal/mol) with T$_1$ in D_{2h} symmetry (both phenylenes perpendicular to PtC$_4$, 19.78 kcal/mol) reveals that in T$_1$, there is a significant energy cost (>15 kcal/mol) for twisting both phenylenes out of the plane relative to PtC$_4$. This latter finding strongly suggests that the triplet excitation is localized on a single phenylene unit, and there is a strong interaction between the excited ligand and the metal center in T$_1$ that is influenced by the relative orientation of the ring with respect to the PtC$_4$ plane.

DISCUSSION

This study reports the synthesis of a range of 11 complexes of the type *trans*-(NHC)$_2$Pt(CC-Ar)$_2$ by a common synthetic protocol that involves the initial formation of the *trans*-(NHC)$_2$PtCl$_2$ complex via transmetallation from the corresponding Ag(I)−NHC complex. The final aryl acetylide complexes are generally obtained in high yields by Hagihara

DOI: 10.1021/acs.jpca.9b07079
J. Phys. Chem. A 2019, 123, 9069−9078

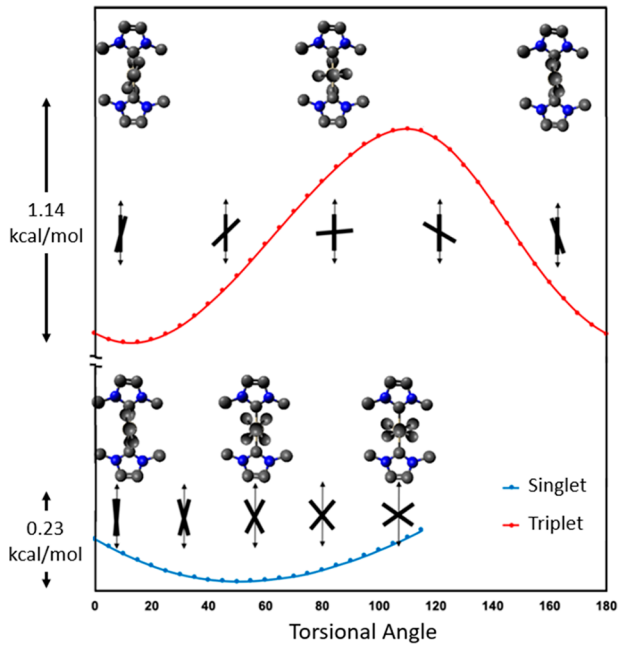

Figure 7. Potential energy surfaces calculated by DFT for structures differing with respect to the torsional angle between the two phenylene ligands of IPtP in the singlet (S_0) and triplet (T_1) states. The molecular conformations are illustrated with the ball−stick models (hydrogens removed for clarity), with a view along the CC−Pt−CC− axis (where CC is the acetylide bond). The stick structures also represent the conformations, with arrows representing the NHC ligands (axial orientation), and the bold lines represent Newman projections of the phenylene rings.

coupling reactions, except in one case where the reaction of the Li-acetylide gave improved yields. Overall, the transmetallation/Hagihara approach gives the target complexes in moderate to high yields under comparatively mild reaction conditions. The reactions are scalable, allowing multigram quantities of the complexes to be obtained.

Detailed photophysical investigations reveal a number of interesting trends. All of the complexes exhibit a strong to moderate ambient temperature phosphorescence from a (spin−orbit mixed) triplet excited state. In this respect, the complexes are similar to a large number of platinum(II) acetylide complexes that have been previously reported to exhibit phosphorescence.[8] However, it is notable that these NHC complexes are phosphorescent at room temperature, whereas structurally similar complexes with phosphine ligands are not emissive.[2] This points to the importance of the strong-field NHC ligands in raising the energy of nonemissive metal-centered (d−d) excited states (vide infra).

This study has explored the effect of exchanging the NHC and aryl acetylide ligands on the phosphorescence. First, there is little effect of changing the NHC ligand from imidazole (Im) to benzimidazole (BIm); Im and BIm complexes with corresponding acetylide ligands have comparable photophysical parameters. By contrast, there are significant variations seen in emission energy, lifetime and phosphorescence yield as the arylacetylide ligand is varied (there is nearly a 0.3 eV variation in E_{em} across the series). This reflects the fact that the triplet excitation is localized on the aryl acetylide ligands. Close inspection of emission data does not reveal any defined trends in E_{em} with the nature of the substituents; the largest shift to lower energy is seen for the $-CF_3$ and −CN substituents, both of which are electron withdrawing. This could reflect a small contribution of MLCT character to the triplet state.

As noted above, the most noticeable trend in the data is the correlation between the emission quantum yield and E_{em}, and the lifetime studies allow us to identify the source of the variation as arising from an increase in the nonradiative decay rate with E_{em}. This effect is pronounced, for the series of Im complexes, there is a ∼80-fold variation in the emission quantum yield and this is accounted for by ∼100-fold variation in the nonradiative decay rate. The temperature-dependent lifetime studies for IPtPyr, $IPtPCF_3$, and IPtPCN show that there is a thermally activated process that dominates the decay of the triplet state at temperatures above 130 K. This process is very likely due to crossing to a d−d excited state, which lies just above the emitting triplet state (see Figure 8). The

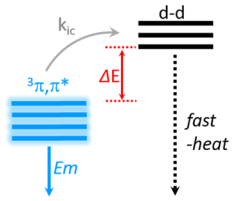

Figure 8. Thermally activated crossing from the phosphorescent triplet state to the d−d excited state.

temperature dependence studies reveal activation energies close to 1000 cm^{-1}. Similar thermally activated quenching of an emitting MLCT excited state has been reported for d^6 Ru−polypyridine complexes, and in these systems, activation energies in the range 1000−3000 cm^{-1} are found.[33]

Although we do not have direct evidence for the existence of the dd state in the present study, there are good reasons to believe that it exists. In particular, ligand field theory predicts that for square planar d^8 metal ions (e.g., $Pt(II)L_4$), the lowest-energy metal-centered states arise from transitions from filled d levels to the empty d_{x2-y2} level.[39] Because the dd transitions are symmetry forbidden, they are not easily observed in the absorption spectra of the complexes reported here due to the allowed π,π^* transitions. Time-dependent density functional theory (TD-DFT) calculations on IPtP do not reveal excitations that can be definitively attributed to metal-centered dd transitions. However, TD-DFT calculations on structurally related square planar Pt(II) complexes with heterocyclic ligands give a clear indication of a transition arising from a metal-centered excitation involving molecular orbitals which are mainly metal centered with approximate transition energy of 3.7 eV.[40]

Variable temperature emission experiments reveal the existence of multiple emitting states in the low-temperature frozen solvent glass. Similar effects have been previously reported for Pt−aryl acetylide complexes and, in those cases, attributed to emission from different conformers resulting from torsions of the phenylene rings.[34,41] In the current study, the energy difference between the onsets of the two emission progressions is ∼0.15 eV (3 kcal/mol). The DFT results are in accord with this difference, suggesting that torsion of one of the phenylenes modulates the triplet energy in the range of a few kcal/mol. Dynamics observed in the ultrafast transient absorption on the time scale of 25 ps likely also corresponds to relaxation in the triplet state associated with torsion of the phenylene units.

DOI: 10.1021/acs.jpca.9b07079
J. Phys. Chem. A 2019, 123, 9069−9078

Finally, as noted in the introduction, one of the current interest in phosphorescent Pt(II) complexes is their potential application as emitters for deep blue OLED application. We have already demonstrated the use of IPtP in vacuum-processed OLED with a maximum external quantum efficiency of 8%.[13] The present study reveals other potentially interesting complexes with blue emission, reasonable quantum yields, and emission lifetimes > 1.5 us, which may have potential to further application in OLED. Preliminary work on these complexes in a glassy polymer matrix shows that emission yields are enhanced significantly in the solid state, suggesting that these will be useful phosphors. Work in progress is investigating the application of this family of phosphors in OLEDs, and the results will be reported separately.

SUMMARY AND CONCLUSIONS

In this work, we have expanded the synthetic possibilities for efficiently accessing strongly blue phosphorescent Pt(II) acetylide complexes. Studies on the emission energy dependence of the photophysics point to a nonemissive d−d excited state as being responsible for quenching of the emission. The strong-field NHC ligands clearly are able to enhance the emission yields by raising the energy of the d−d excited state compared to its position in the structurally analogous phosphine complexes. However, although the NHC ligands do increase the energy of the d−d state, it can still be thermally populated and is a significant contribution to the nonradiative decay and quenching of the emission at an ambient temperature. Some of the complexes investigated here have promising emission properties that may be useful in OLED application, and this will be explored in-depth in a forthcoming report.

EXPERIMENTAL SECTION

Synthesis and Structure. Details on the synthesis and characterization of platinum complexes are given in the Supporting Information.

Photophysical Measurements. UV−visible absorption spectra were obtained on a Shimadzu UV-1800 dual-beam spectrophotometer. Steady-state photoluminescence measurements were performed on a Horiba Fluorolog-3 spectrophotometer with a xenon arc lamp and Horiba photomultiplier tube (detector range: 290−850 nm). Phosphorescence lifetime measurements were accomplished for $IPtPCF_3$, IPtPyr, and IPtPCN using an in-house apparatus with a Continuum Surelite II series Nd:YAG laser (3rd harmonic λ = 355 nm, 1.5 mJ per pulse) as the excitation source. Phosphorescent lifetimes for the remaining compounds were recorded with a PicoQuant FluoTime 300 Fluorescence Lifetime Spectrophotometer by the time-correlated single-photon counting (TCSPC) technique (PicoQuant Time Harp module). In this system, a Ti:Saphire Coherent Chameleon Ultra laser was used as the excitation source. The Chameleon laser provides pulses of 80 MHz that can be tuned from 680 to 1080 nm. The 80 MHz pulse train was sampled using a Coherent Model 9200 pulse picker to provide excitation pulses at an acceptable repetition rate and was frequency-doubled using a Coherent second harmonic generator. An excitation wavelength of 340 nm was chosen for all samples.

Temperature-dependent measurements were performed in a Fluorolog-3 spectrometer for the steady-state measurements and the Continuum Surelite laser for the time-resolved measurements. The variable temperature measurements were carried out by cooling samples in an OptistatDN variable liquid nitrogen cryostat (Oxford Instruments). The optical density of the samples was adjusted to approximately 0.2 at the excitation wavelength utilizing 2-methyltetrahydrofuran as the solvent. The samples were deoxygenated by a minimum of five freeze pump thaw cycles.

Femtosecond transient absorption data were collected using pump−probe techniques with a 120 fs, 1 kHz Ti:sapphire (Coherent Astrella) laser. The pump beam was generated using a portion of the 800 nm amplifier beam by being directed into an Opera Solo (Coherent) OPA, which was tuned to generate a beam of light of 330 nm. The pump beam was then directed into a Helios Fire (Ultrafast Systems) automated femtosecond transient absorption spectrometer where the beam passed through a mechanical chopper, depolarizer, and neutral density filter to tune the beam to 0.1 mW (100 nJ/pulse) of power before hitting the stirred sample (0.2 O.D.). Another portion of the 800 nm beam was directed into the Helios Fire directed into an automated 8 ns delay stage, afterward, the beam was focused into a calcium fluoride crystal to generate a visible probe ranging from 420 to 700 nm. The visible signal was detected using a fiber-coupled alignment-free spectrometer with a 1024 pixel CMOS sensor. The time delay between the pump and probe is controlled using the computer-software-controlled delay stage that has an approximate time resolution of 250 fs.

Computational Methods. All calculations were performed with the Gaussian 09 (Revision D.01) suite of software using DFT methods. To mitigate computational costs, the cyclohexane moieties of IPtP were replaced with methyl groups and calculations were done in a vacuum. Singlet (S_0) and triplet (T_1) geometries were optimized using the B3LYP functional in conjunction with the SDD basis set for all atoms, as described in the previous work. To better understand the allowable conformations of the excited triplet state, further optimizations were done while maintaining forced point group symmetry. These optimized geometries and their relative energies with respect to the symmetry-unrestricted minimum are shown in Figure S39.

Torsional potential energy surfaces were generated by first setting the dihedral angle between the rings of the phenylene ligands to 0° and co-planar with PtC_4. The geometry of IPtP was then relaxed using the described optimization methodology. The torsion between phenylene rings was fixed throughout this optimization process, while all other degrees of freedom were not, including phenylene torsions relative to PtC_4. The inter-ring dihedral was increased by steps of 5 degrees, and the geometry reoptimized at every step for a total of 360° of rotation. These calculations were done with symmetry constraints disabled.

ASSOCIATED CONTENT

Supporting Information

The Supporting Information is available free of charge on the ACS Publications website at DOI: 10.1021/acs.jpca.9b07079.

Complete details concerning the synthesis and characterization of all new compounds, ^1H and ^{13}C NMR spectra, tables of X-ray data and additional photophysical results (PDF)

Crytallographic data of BiPP (CIF)

Crytallographic data of $BIPtCl_2$ (CIF)

DOI: 10.1021/acs.jpca.9b07079
J. Phys. Chem. A 2019, 123, 9069−9078

AUTHOR INFORMATION

Corresponding Author

*Email: kirk.schanze@utsa.edu. Web: http://SchanzeLab.org.

ORCID

Silvano R. Valandro: 0000-0002-4652-768X
Charles J. Zeman, IV: 0000-0001-5275-0469
Kirk S. Schanze: 0000-0003-3342-4080

Author Contributions

§J.D.B. and S.R.V. contributed equally to this work.

Notes

The authors declare no competing financial interest.

ACKNOWLEDGMENTS

This work was supported by the National Science Foundation (Grant No. CHE-1737714). K.S.S. also acknowledges the Welch Foundation for support through the Welch Chair at the University of Texas at San Antonio (Award No. AX-0045-20110629).

REFERENCES

(1) Rogers, J. E.; Hall, B. C.; Hufnagle, D. C.; Slagle, J. E.; Ault, A. P.; McLean, D. G.; Fleitz, P. A.; Cooper, T. M. Effect of Platinum on the Photophysical Properties of a Series of Phenyl-Ethynyl Oligomers. *J. Chem. Phys.* **2005**, *122*, No. 214708.

(2) Rogers, J. E.; Cooper, T. M.; Fleitz, P. A.; Glass, D. J.; McLean, D. G. Photophysical Characterization of a Series of Platinum(II)-Containing Phenyl-Ethynyl Oligomers. *J. Phys. Chem. A* **2002**, *106*, 10108−10115.

(3) Cooper, T. M.; Krein, D. M.; Burke, A. R.; McLean, D. G.; Rogers, J. E.; Slagle, J. E.; Fleitz, P. A. Spectroscopic Characterization of a Series of Platinum Acetylide Complexes Having a Localized Triplet Exciton. *J. Phys. Chem. A* **2006**, *110*, 4369−4375.

(4) Cooper, T. M.; Krein, D. M.; Burke, A. R.; McLean, D. G.; Rogers, J. E.; Slagle, J. E. Asymmetry in Platinum Acetylide Complexes: Confinement of the Triplet Exciton to the Lowest Energy Ligand. *J. Phys. Chem. A* **2006**, *110*, 13370−13378.

(5) Silverman, E. E.; Cardolaccia, T.; Zhao, X.; Kim, K.-Y.; Haskins-Glusac, K.; Schanze, K. S. The Triplet State in Pt-Acetylide Oligomers, Polymers and Copolymers. *Coord. Chem. Rev.* **2005**, *249*, 1491−1500.

(6) Köhler, A.; Wilson, J. Phosphorescence and Spin-Dependent Exciton Formation in Conjugated Polymers. *Org. Electron.* **2003**, *4*, 179−189.

(7) Wong, W.-L.; Ho, C.-L. Di-, Oligo- and Polymetallaynes: Syntheses, Photophysics, Structures and Applications. *Coord. Chem. Rev.* **2006**, *250*, 2627−2690.

(8) Yam, V. W.-W.; Au, V. K.-M.; Leung, S. Y.-L. Light-Emitting Self-Assembled Materials Based on D8 and D10 Transition Metal Complexes. *Chem. Rev.* **2015**, *115*, 7589−7728.

(9) Zieba, R.; Desroches, C.; Chaput, F.; Carlsson, M.; Eliasson, B.; Lopes, C.; Lindgren, M.; Parola, S. Preparation of Functional Hybrid Glass Material from Platinum (II) Complexes for Broadband Nonlinear Absorption of Light. *Adv. Funct. Mater.* **2009**, *19*, 235−241.

(10) Westlund, R.; Malmström, E.; Lopes, C.; Öhgren, J.; Rodgers, T.; Saito, Y.; Kawata, S.; Glimsdal, E.; Lindgren, M. Efficient Nonlinear Absorbing Platinum (II) Acetylide Chromophores in Solid PMMA Matrices. *Adv. Funct. Mater.* **2008**, *18*, 1939−1948.

(11) Shelton, A. H.; Price, R. S.; Brokmann, L.; Dettla, B.; Schanze, K. S. High Efficiency Platinum Acetylide Nonlinear Absorption Chromophores Covalently Linked to Poly(Methyl Methacrylate). *ACS Appl. Mater. Interfaces* **2013**, *5*, 7867−7874.

(12) Dubinina, G. G.; Price, R. S.; Abboud, K. A.; Wnuk, P.; Stepanenko, Y.; Drobizhev, M.; Rebane, A.; Schanze, K. S. Phenylene Vinylene Platinum(II) Acetylides with Prodigious Two- Photon Absorption. *J. Am. Chem. Soc.* **2012**, *134*, 19346−19349.

(13) Bullock, J. D.; Salehi, A.; Zeman, C. J. I.; Abboud, K. A.; So, F.; Schanze, K. S. In Search of Deeper Blues: Trans-N-Heterocyclic Carbene Platinum Phenylacetylide as a Dopant for Phosphorescent OLEDs. *ACS Appl. Mater. Interfaces* **2017**, *9*, 41111−41114.

(14) Zhang, Y.; Blacque, O.; Venkatesan, K. Highly Efficient Deep-Blue Emitters Based on Cis and Trans N-Heterocyclic Carbene PtIIacetylide Complexes: Synthesis, Photophysical Properties, and Mechanistic Studies. *Chem. - Eur. J.* **2013**, *19*, 15689−15701.

(15) Williams, J. A. G.; Rochester, D. L.; Murphy, L. Optimising the Luminescence of Platinum(II) Complexes and Their Application in Organic Light Emitting Devices (OLEDs). *Coord. Chem. Rev.* **2008**, *252*, 2596−2611.

(16) Westlund, R.; Glimsdal, E.; Lindgren, M.; Vestberg, R.; Hawker, C.; Lopes, C.; Malmström, E. Click Chemistry for Photonic Applications: Triazole-Functionalized Platinum (II) Acetylides for Optical Power Limiting. *J. Mater. Chem.* **2008**, *18*, 166−175.

(17) Price, R. S.; Dubinina, G.; Drobizhev, M.; Rebane, A.; Schanze, K. S. Polymer Monoliths Containing Two-Photon Absorbing Phenylenevinylene Platinum(II) Acetylide Chromophores for Optical Power Limiting. *ACS Appl. Mater. Interfaces* **2015**, *7*, 10795−10805.

(18) Guo, F.; Kim, Y.-G.; Reynolds, J. R.; Schanze, K. S. Platinum−Acetylide Polymer Based Solar Cells: Involvement of the Triplet State for Energy Conversion. *Chem. Commun.* **2006**, 1887−1889.

(19) Mei, J.; Ogawa, K.; Kim, Y.-G.; Heston, N. C.; Arenas, D. J.; Nasrollahi, Z.; McCarley, T. D.; Tanner, D. B.; Reynolds, J. R.; Schanze, K. S. Low-Band-Gap Platinum Acetylide Polymers as Active Materials for Organic Solar Cells. *ACS Appl. Mater. Interfaces* **2009**, *1*, 150−161.

(20) Guo, F.; Ogawa, K.; Kim, Y.-G.; Danilov, E. O.; Castellano, F. N.; Reynolds, J. R.; Schanze, K. S. A Fulleropyrrolidine End-Capped Platinum-Acetylide Triad: The Mechanism of Photoinduced Charge Transfer in Organometallic Photovoltaic Cells. *Phys. Chem. Chem. Phys.* **2007**, *9*, 2724−2734.

(21) Chatt, J.; Shaw, B. L. Alkyls and Aryls of Transition Metals. Part II. Platinum(II) Derivatives. *J. Chem. Soc.* **1959**, 4020−4033.

(22) Williams, J. A. G. Topics in Current Chemistry: Photochemistry and Photophysics of Coordination Compounds. In *Topics in Current Chemistry*; Springer: Heidelberg, 2007; pp 205−268.

(23) Bourissou, D.; Guerret, O.; Gabbaï, F. P.; Bertrand, G. Stable Carbenes. *Chem. Rev.* **2000**, *100*, 39−92.

(24) Badley, E. M.; Chatt, J.; Richards, R. L.; Sim, G. A. The Reactions of Isocyanide Complexes of Platinum(II): A Convenient Route to Carbene Complexes. *J. Chem. Soc. D* **1969**, 1322−1323.

(25) Tenne, M.; Unger, Y.; Strassner, T. (Acetylacetonato-K2O,O′)[1-(4-Bromophenyl-KC 2)-3-Methylimidazol-2-Ylidene-KC 2]Platinum(II). *Acta Crystallogr., Sect. C: Cryst. Struct. Commun.* **2012**, *68*, m203−m205.

(26) Tronnier, A.; Pöthig, A.; Metz, S.; Wagenblast, G.; Münster, I.; Strassner, T. Enlarging the π System of Phosphorescent (C^C*) Cyclometalated Platinum(II) NHC Complexes. *Inorg. Chem.* **2014**, *53*, 6346−6356.

(27) Zhang, Y.; Garg, J. A.; Michelin, C.; Fox, T.; Blacque, O.; Venkatesan, K. Synthesis and Luminescent Properties of Cis Bis-N-Heterocyclic Carbene Platinum(II) Bis-Arylacetylide Complexes. *Inorg. Chem.* **2011**, *50*, 1220−1228.

(28) Zhang, Y.; Clavadetscher, J.; Bachmann, M.; Blacque, O.; Venkatesan, K. Tuning the Luminescent Properties of Pt(II) Acetylide Complexes through Varying the Electronic Properties of N-Heterocyclic Carbene Ligands. *Inorg. Chem.* **2014**, *53*, 756−771.

(29) Winkel, R. W.; Dubinina, G. G.; Abboud, K. A.; Schanze, K. S. Photophysical Properties of Trans-Platinum Acetylide Complexes Featuring N-Heterocyclic Carbene Ligands. *Dalton Trans.* **2014**, *43*, 17712−17720.

(30) Zhang, Y. Z.; Hauke, C. E.; Crawley, M. R.; Schurr, B. E.; Fulong, C. R. P.; Cook, T. R. Increasing Phosphorescent Quantum Yields and Lifetimes of Platinum-Alkynyl Complexes with Extended Conjugation. *Dalton Trans.* **2017**, *46*, 9794−9800.

(31) If there is a dark state that is above the emitting state by an amount of energy ΔE, then a linear correlation will be observed

DOI: 10.1021/acs.jpca.9b07079
J. Phys. Chem. A 2019, 123, 9069−9078

between the non-radiative decay rate and energy gap as follows: $\ln k_{nr} = E_{em}/RT + C$. This follows from the Arrhenius equation where it assumed that the energy of the dark state does not vary across the series. This equation predicts a linear correlation between $\ln k_{nr}$ and emission energy with a slope equal to $1/RT$ (which is 38.7 eV^{-1} at 300 K).

(32) Caspar, J. V.; Meyer, T. J. Application of the Energy Gap Law to Nonradiative, Excited-State Decay. *J. Phys. Chem. A* **1983**, *87*, 952−957.

(33) Wacholtz, W. F.; Auerbach, R. A.; Schmehl, R. H. Independent Control of Charge-Transfer and Metal-Centered Excited States in Mixed-Ligand Polypyridine Ruthenium(II) Complexes via Specific Ligand Design. *Inorg. Chem.* **1986**, *25*, 227−234.

(34) Glusac, K.; Köse, M. E.; Jiang, H.; Schanze, K. S. Triplet Excited State in Platinum-Acetylide Oligomers: Triplet Localization and Effects of Conformation. *J. Phys. Chem. B* **2007**, *111*, 929−940.

(35) Van Houten, J.; Watts, R. J. Temperature Dependence of the Photophysical and Photochemical Properties of the Tris(2,2′-Bipyridyl)Ruthenium(II) Ion in Aqueous Solution. *J. Am. Chem. Soc.* **1976**, *98*, 4853−4858.

(36) Wang, Y.; Schanze, K. S. Intramolecular Energy Transfer in (Diimine)$Re^{I}(CO)_3$-[CpM^{II}(Arene)] Dimers. *Inorg. Chem.* **1994**, *33*, 1354−1362.

(37) Ramakrishna, G.; Goodson, T., III; Rogers-Haley, J. E.; Cooper, T. M.; McLean, D. G.; Urbas, A. Ultrafast Intersystem Crossing: Excited State Dynamics of Platinum Acetylide Complexes. *J. Phys. Chem. C* **2009**, *113*, 1060−1066.

(38) Foresman, J.; Frisch, A. *Exploring Chemistry with Electronic Structure Methods*, 2nd ed.; Gaussian: Pittsburgh, 1996.

(39) Cotton, F. A. *Chemical Applications of Group Theory*, 3rd ed.; Wiley-Interscience: NY, 1990.

(40) Huff, G. S. Excited States of d^6 and d^8 Transition Metal Complexes. Ph.D. Dissertation; University of Otago, 2017. https://ourarchive.otago.ac.nz/handle/10523/7155 (accessed Sept 09, 2019).

(41) Lin, C. J.; Chen, C. Y.; Kundu, S. K.; Yang, J. S. Unichromophoric Platinum-Acetylides That Contain Pentiptycene Scaffolds: Torsion-Induced Dual Emission and Steric Shielding of Dynamic Quenching. *Inorg. Chem.* **2014**, *53*, 737−745.

DOI: 10.1021/acs.jpca.9b07079
J. Phys. Chem. A 2019, 123, 9069−9078